

IUE Low Dispersion Sensitivity Monitoring XV.

Introduction

The low dispersion sensitivity monitoring analysis for the LWP and SWP cameras has been updated to August 1988. Updates to the LWR data base have stopped as image processing for that camera with the new VAX computer has been delayed. A preliminary analysis of the LWP sensitivity monitoring data, reprocessed with the new ITF, and a comparison with the old ITF data, is included in this report. The following stars are used to monitor changes in camera sensitivity:

BD+28° 4211, HD 93521, HD60753, BD+33° 2642, BD+75° 325.

The symbols for each star are, respectively:

+ , * , ◊ , □ , Δ .

Analysis

The sensitivity data are analyzed using the standard methods as described by Holm and Schiffer (1980). The data are ratioed to a reference spectrum for each star and placed into three wavelength bins, each 150Å wide (300Å for the LWR). The binned flux ratios are then fit with a multiple linear regression to find the rate of change (%/yr.) in each wavelength region and the overall temperature dependence (%/°C) of the camera. The temperature dependence is assumed to be time independent and is fit to the head amplifier temperature (THDA). The LWP camera uses six wavelength bins and the flux, instead of being ratioed to a reference spectrum, is normalized to the maximum flux before being fit with the regression. The fifth standard, BD+75° 325, is not included in the SWP sensitivity monitoring analysis. The temperature and time dependent coefficients for the three cameras are listed in Table 1. The data are normalized to 1978 and corrected for camera temperature (THDA) dependence before being plotted in Figures 1-4.

Results

The SWP data, as plotted in Figure 4, exhibit little change over previous values.

The results of the LWP data are plotted in Figures 1 and 2. The 2900Å wavelength region shows an essentially zero sensitivity degradation, while the other regions show little change over previous values (i.e. the differences are well within the standard deviations). Both the time and temperature dependent coefficients, as shown in Table 1, are significantly lower than those for the other cameras. A noticeable jump in sensitivity at the end of 1987, which is mainly visible in the last two wavelength regions, is probably due to the switch to the new ITF and absolute calibration.

The camera head amplifier temperatures (THDA) are also monitored for temporal variations and are plotted in Figure 5. The average THDA values for the three cameras are:

$$\begin{aligned} \text{LWP (1988.7)} &= 9.8 \text{ }^\circ\text{C} \\ \text{LWR (1988.1)} &= 14.6 \text{ }^\circ\text{C} \\ \text{SWP (1988.7)} &= 9.8 \text{ }^\circ\text{C} \end{aligned}$$

There is little statistical evidence for the camera temperatures increasing with time when the least-squares analysis is restricted to dates after 1981 (1983 for the LWP).

LWP Sensitivity Degradation with the New Calibration

The IUE project plans to reprocess the entire IUE archives with the best processing methods and calibrations possible. A correction for camera sensitivity degradation has been proposed to be included in the calibrations for the final processing effort (Imhoff, et al., 1988). This is necessary because sensitivity degradation can contribute significant errors to the derived extracted fluxes (up to about 15% for the LWR camera).

A sensitivity correction method similar to the study of Clavel, Gilmozzi, and Prieto (1986) could be used for the final processing. We propose that the sensitivity correction method, which will be used during the final reprocessing, should have the following characteristics: First, the degradation rates should be derived for the same 25\AA bins as is used for the absolute calibration. Second, the degradation rates should be derived using data processed with the ITF and absolute calibrations most appropriate to that time period. Third, the degradation rates should be determined relative to a zero point, which is tied to the epoch of the ITF and absolute calibrations. Fourth, the degradation rates should be determined for specified time intervals (e.g. 6 months?). This differs from the Clavel technique which derived a polynomial (linear) fit to the sensitivity degradation data. However, as is apparent from Figures 1-4, the camera sensitivity degradation does not always follow a simple linear function. This method potentially can follow the "bumps and wiggles" more accurately than a simple linear fit. Finally, a table of total degradation values as a function of time interval and wavelength bin, along with an interpolation method between time intervals, would be used to correct the extracted fluxes for sensitivity degradation.

Analysis of the LWP sensitivity data, reprocessed with the new ITF, has begun. Forty images for the calibration star HD 93521 were reduced using a slightly different (preliminary) method of analysis than outlined above. The data were first averaged into thirty six (25\AA wide) wavelength bins (Table 2). The data were then binned into six month intervals and a mean coefficient representing the total amount of degradation since 1978.0 was computed for each interval. The mean of the coefficients and their standard deviations, for both the old and new ITF, are shown in Table 3. The differences between the old and new ITF's are very small and in most cases within one standard deviation of the means. Several representative plots of these differences are shown in Figures 6 and 7. At the time of writing, a much larger old ITF data set than new ITF data was available for study.

Once the remaining sensitivity data has been reprocessed with the new ITF and the table has been completed one will be able to apply a correction to the absolute calibration depending upon when ones data were taken. A similar method will eventually be applied to the other two cameras.

Matthew P. Garhart

Nancy A. Oliverson

Terry J. Teays

- Holm, A.V., and Schiffer, F.H., 1980, "IUE Camera Sensitivity Variations", NASA IUE Newsletter No. 9, p. 8
- Garhart, M.P., and Teays, T.J., 1988, "IUE Low Dispersion Sensitivity Monitoring XIV.", NASA IUE Newsletter No. 35, p. 99
- Imhoff, C., Oliverson, N., Nichols-Bohlin, J., Cassatella, A., and Lloyd, C., 1988, "The Recalibration of the IUE Scientific Instrument", A Decade of Astronomy with the IUE Satellite, ESA SP-281, Vol. 2, p. 341
- Clavel, J., Gilmozzi, R., and Prieto, A., 1986, "A Correction Method for the Degradation of the LWR Camera (II): Erratum and Final Results", NASA IUE Newsletter, No. 31, p. 83

Table 1.

Results of low dispersion camera sensitivity analysis - Aug. 1988

LWP CameraTemperature dependence = -0.23 ± 0.02 %/°C

RMS error for a single observation = 3.5 %

333 data points used in regression

Wavelength Region (Å)	Time Dependence (%/yr.)					
	1988.7	1988.4	1987.7	1986.4	1985.3	1984.2
2075 - 2225	-0.12±0.04	-0.05±0.04	+0.07±0.05	+0.20±0.09	+0.29±0.11	-0.09±0.15
2225 - 2375	-0.35±0.04	-0.33±0.04	-0.27±0.05	-0.22±0.09	-0.06±0.11	-0.61±0.15
2375 - 2525	-0.48±0.04	-0.42±0.04	-0.40±0.05	-0.42±0.09	-0.27±0.11	-1.05±0.15
2525 - 2675	-0.59±0.04	-0.55±0.04	-0.59±0.05	-0.48±0.09	-0.13±0.11	-0.84±0.15
2675 - 2825	-0.29±0.04	-0.27±0.04	-0.34±0.05	-0.11±0.09	+0.24±0.11	-0.03±0.15
2825 - 2975	-0.01±0.04	+0.03±0.04	-0.05±0.05	+0.11±0.09	+0.39±0.11	+0.15±0.15

LWR CameraTemperature dependence = -0.82 ± 0.04 %/°C

RMS error for a single observation = 3.5 %

371 data points used in regression

-5.0 kV UVC = 319 data pts.

-4.5 kV UVC = 52 data pts.

Wavelength Region (Å)	Time dependence (%/yr.)					
	1988.1	1987.7	1986.4	1985.3	1984.2	1983.4
2250 - 2550	-2.06±0.04	-2.34±0.05	-2.49±0.08	-2.23±0.10	-2.45±0.09	-2.30±0.11
2550 - 2650	-1.51±0.04	-1.65±0.05	-1.73±0.08	-1.69±0.10	-1.36±0.09	-1.19±0.11
2750 - 3050	-1.34±0.04	-1.55±0.05	-1.73±0.08	-1.84±0.10	-1.35±0.09	-1.13±0.11

SWP CameraTemperature dependence = -0.44 ± 0.03 %/°C

RMS error for a single observation = 3.2 %

366 data points used in regression

Wavelength Region (Å)	Time dependence (%/yr.)					
	1988.7	1987.7	1986.3	1985.3	1984.2	1983.4
1225 - 1375	-0.75±0.04	-0.69±0.04	-0.66±0.06	-0.69±0.08	-0.72±0.13	-0.46±0.16
1475 - 1625	-0.47±0.04	-0.38±0.04	-0.22±0.06	-0.17±0.08	-0.16±0.13	+0.16±0.16
1775 - 1925	-0.79±0.04	-0.78±0.04	-0.69±0.06	-0.63±0.08	-0.86±0.13	-0.63±0.16

Table 2.

WAVELENGTH REGION (ANGSTROMS)
1. 2075 - 2100
2. 2100 - 2125
3. 2125 - 2150
4. 2150 - 2175
5. 2175 - 2200
6. 2200 - 2225
7. 2225 - 2250
8. 2250 - 2275
9. 2275 - 2300
10. 2300 - 2325
11. 2325 - 2350
12. 2350 - 2375
13. 2375 - 2400
14. 2400 - 2425
15. 2425 - 2450
16. 2450 - 2475
17. 2475 - 2500
18. 2500 - 2525
19. 2525 - 2550
20. 2550 - 2575
21. 2575 - 2600
22. 2600 - 2625
23. 2625 - 2650
24. 2650 - 2675
25. 2675 - 2700
26. 2700 - 2725
27. 2725 - 2750
28. 2750 - 2775
29. 2775 - 2800
30. 2800 - 2825
31. 2825 - 2850
32. 2850 - 2875
33. 2875 - 2900
34. 2900 - 2925
35. 2925 - 2950
36. 2950 - 2975

Table 4.

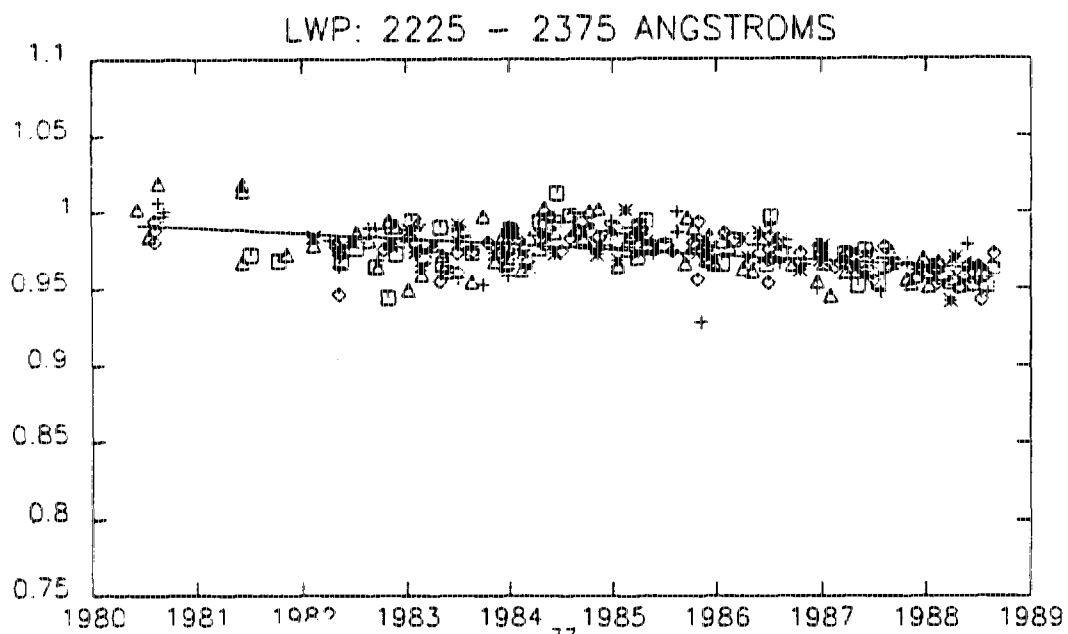
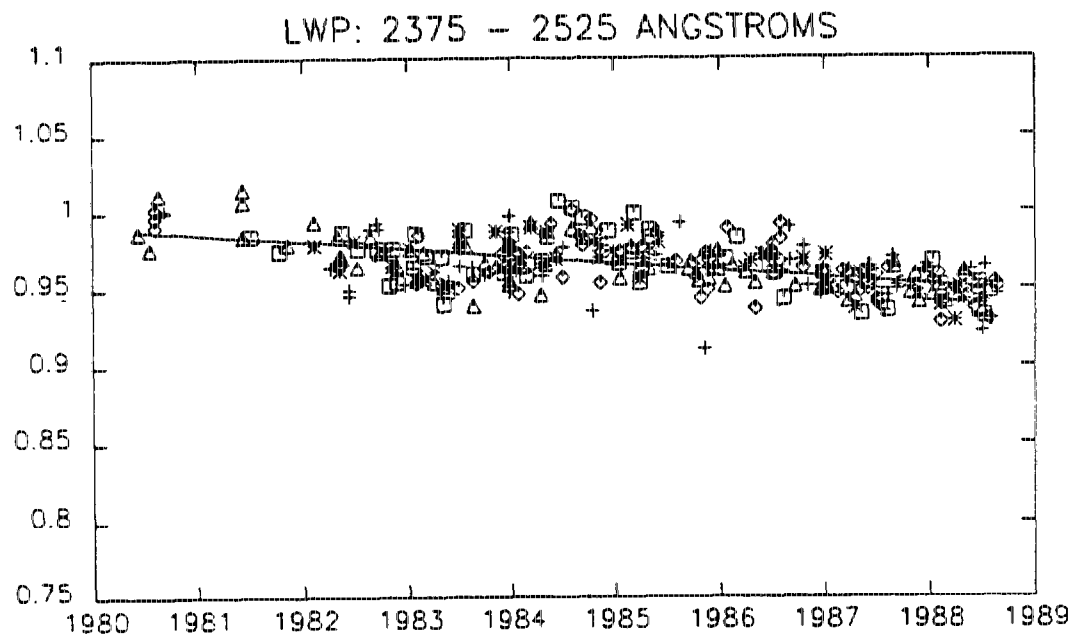
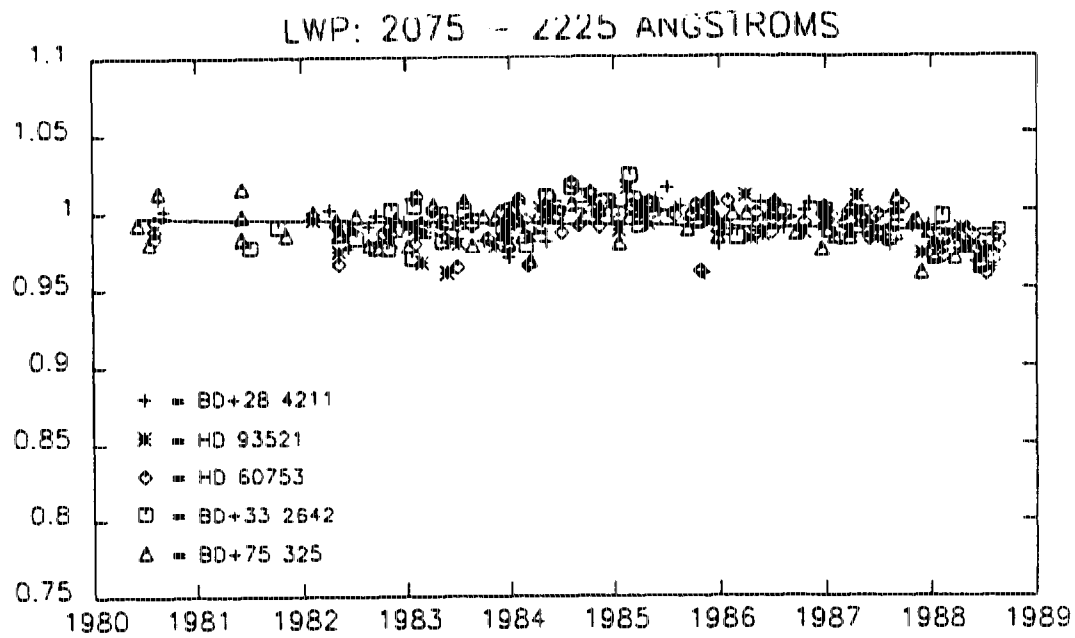
OLD ITF

1	...
2	...
3	...
4	...
5	...
6	...
7	...
8	...
9	...
10	...
11	...
12	...
13	...
14	...
15	...
16	...
17	...
18	...
19	...
20	...
21	...
22	...
23	...
24	...
25	...
26	...
27	...
28	...
29	...
30	...
31	...
32	...
33	...
34	...
35	...
36	...
37	...
38	...
39	...
40	...
41	...
42	...
43	...
44	...
45	...
46	...
47	...
48	...
49	...
50	...
51	...
52	...
53	...
54	...
55	...
56	...
57	...
58	...
59	...
60	...
61	...
62	...
63	...
64	...
65	...
66	...
67	...
68	...
69	...
70	...
71	...
72	...
73	...
74	...
75	...
76	...
77	...
78	...
79	...
80	...
81	...
82	...
83	...
84	...
85	...
86	...
87	...
88	...
89	...
90	...
91	...
92	...
93	...
94	...
95	...
96	...
97	...
98	...
99	...
100	...

NEW ITF

1	...
2	...
3	...
4	...
5	...
6	...
7	...
8	...
9	...
10	...
11	...
12	...
13	...
14	...
15	...
16	...
17	...
18	...
19	...
20	...
21	...
22	...
23	...
24	...
25	...
26	...
27	...
28	...
29	...
30	...
31	...
32	...
33	...
34	...
35	...
36	...
37	...
38	...
39	...
40	...
41	...
42	...
43	...
44	...
45	...
46	...
47	...
48	...
49	...
50	...
51	...
52	...
53	...
54	...
55	...
56	...
57	...
58	...
59	...
60	...
61	...
62	...
63	...
64	...
65	...
66	...
67	...
68	...
69	...
70	...
71	...
72	...
73	...
74	...
75	...
76	...
77	...
78	...
79	...
80	...
81	...
82	...
83	...
84	...
85	...
86	...
87	...
88	...
89	...
90	...
91	...
92	...
93	...
94	...
95	...
96	...
97	...
98	...
99	...
100	...

Figure 1.



LWP: 2525 - 2675 ANGSTROMS

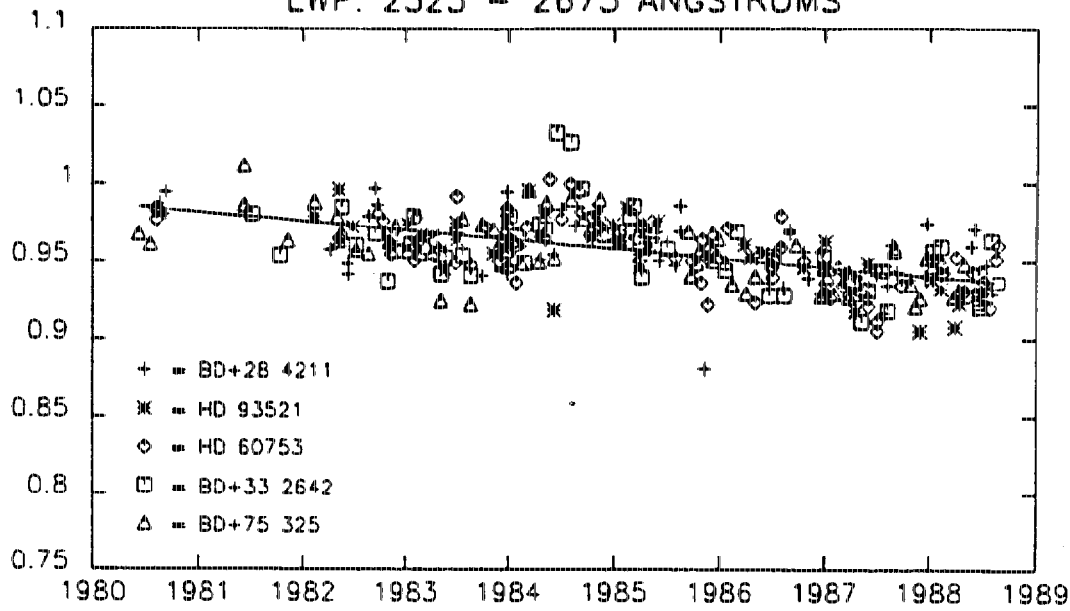
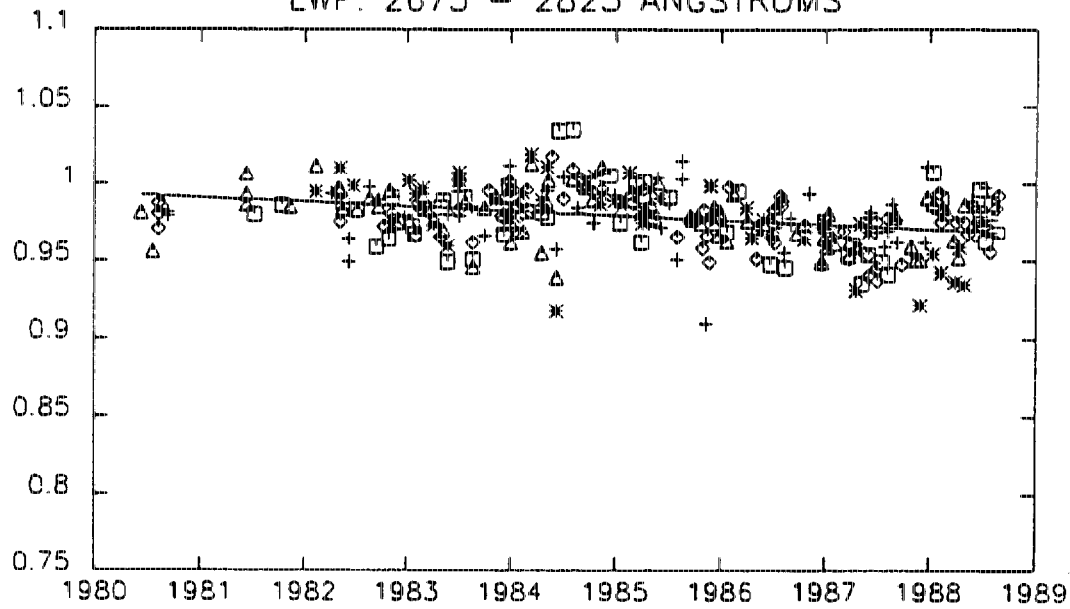


Figure 2.

LWP: 2675 - 2825 ANGSTROMS



LWP: 2825 - 2975 ANGSTROMS

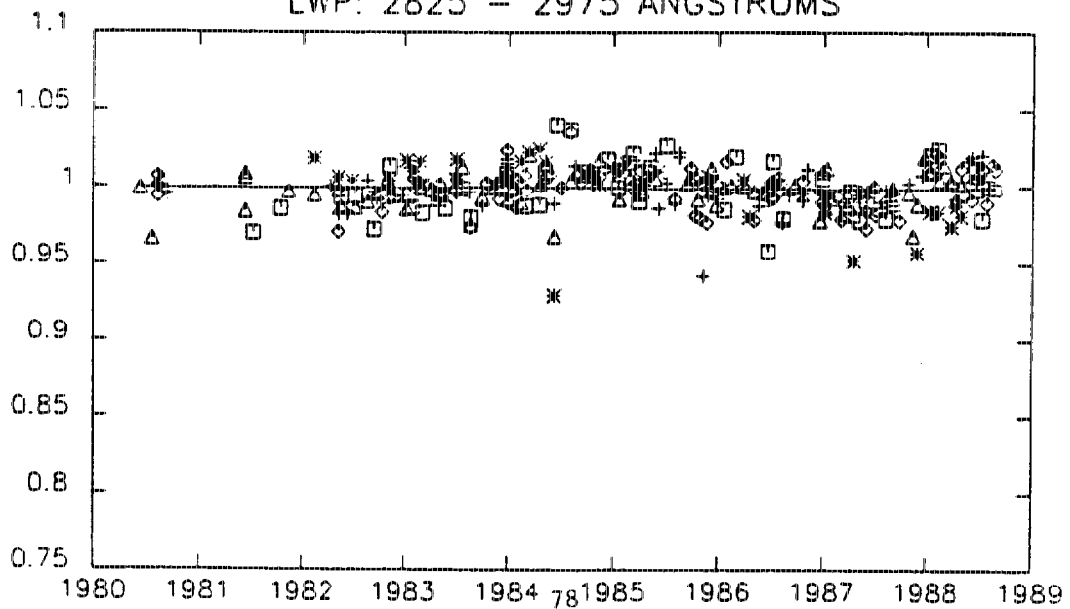
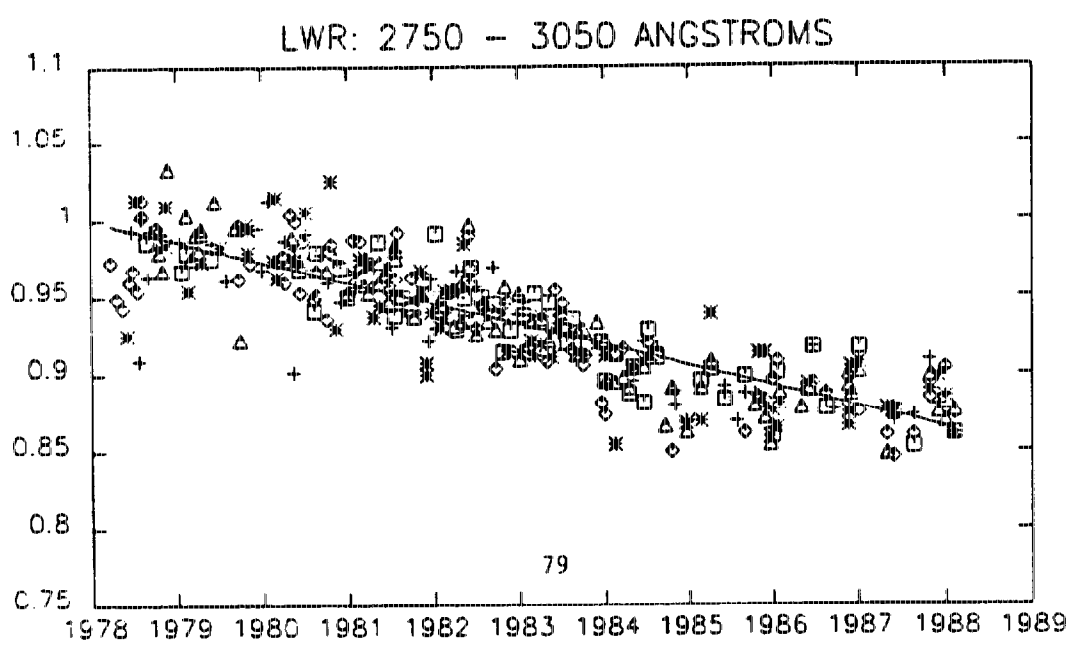
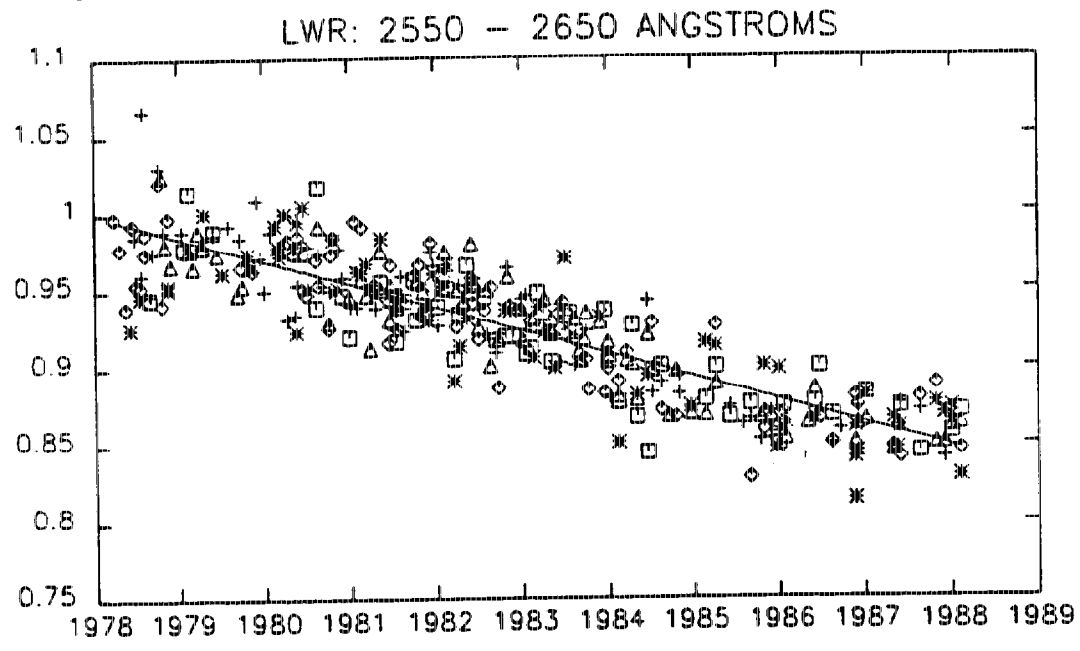
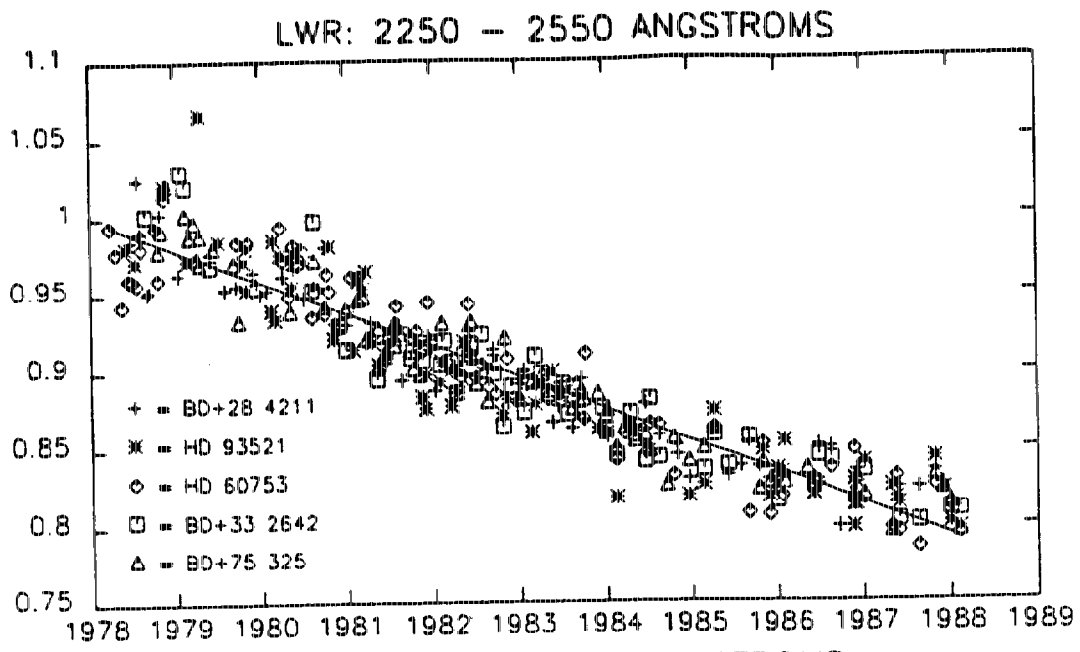


Figure 3.



SWP: 1225 - 1375 ANGSTROMS

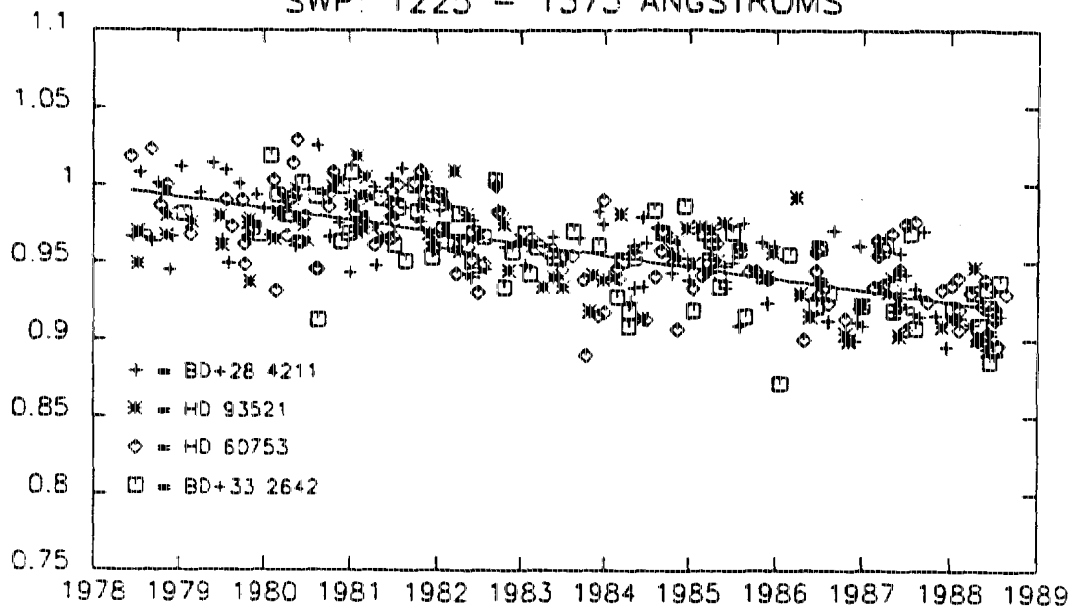
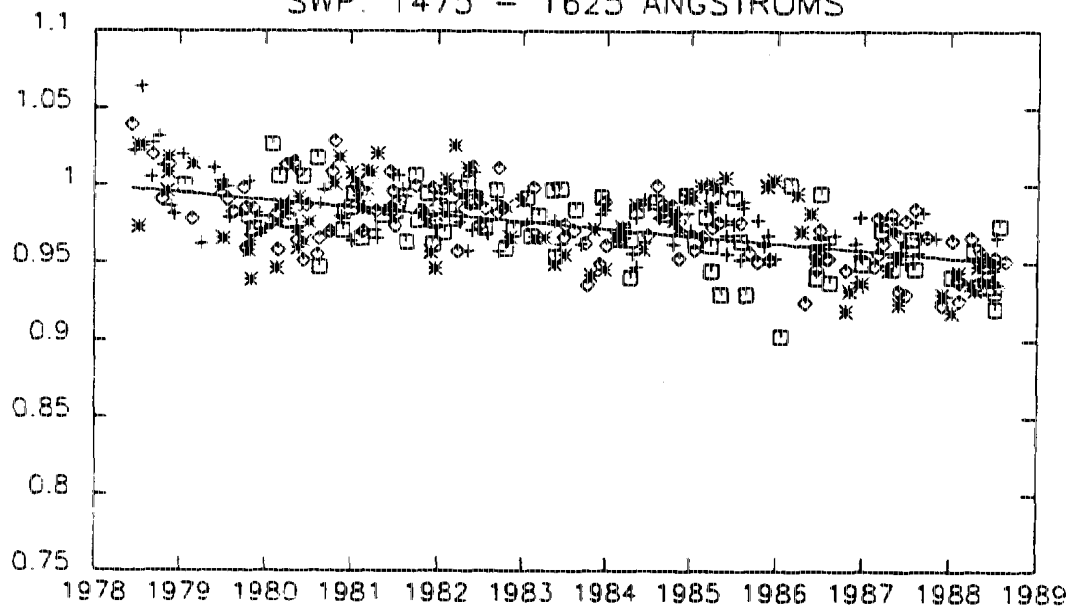
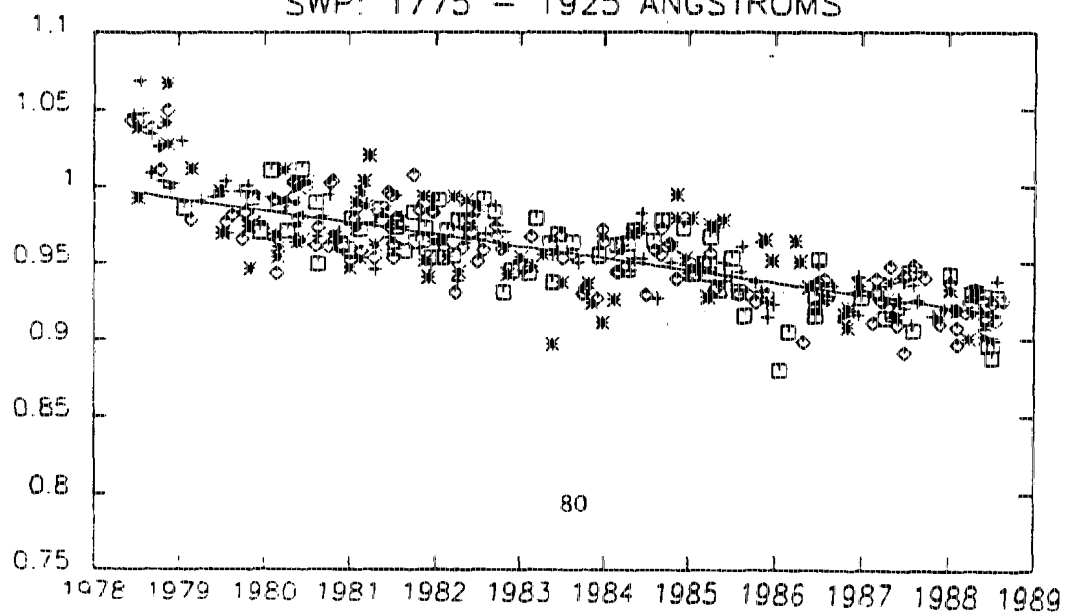


Figure 4.

SWP: 1475 - 1625 ANGSTROMS



SWP: 1775 - 1925 ANGSTROMS



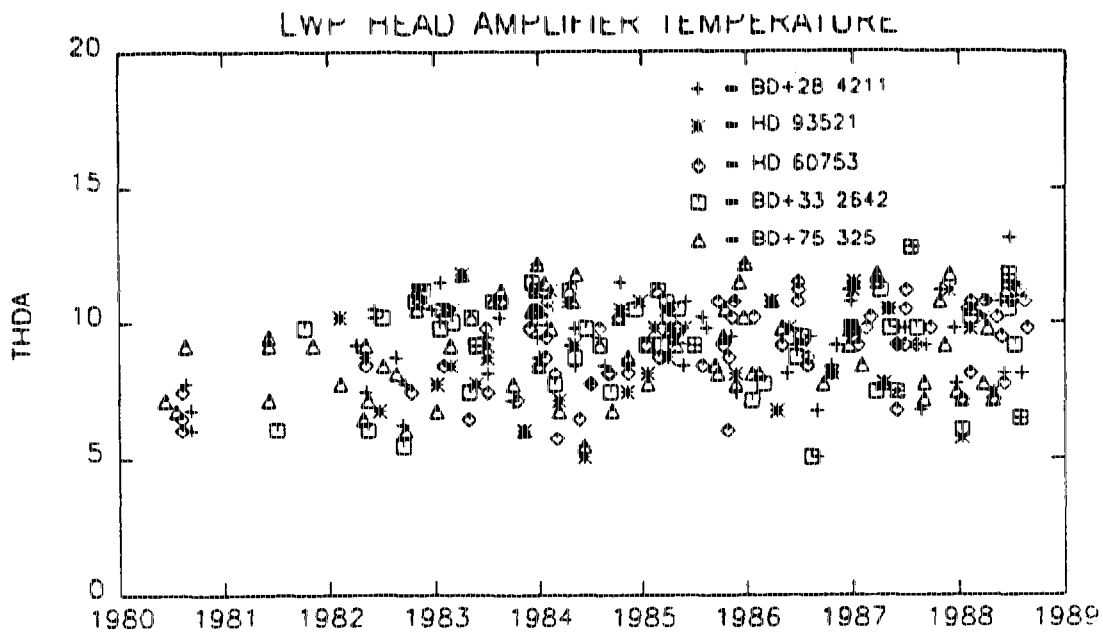


Figure 5.

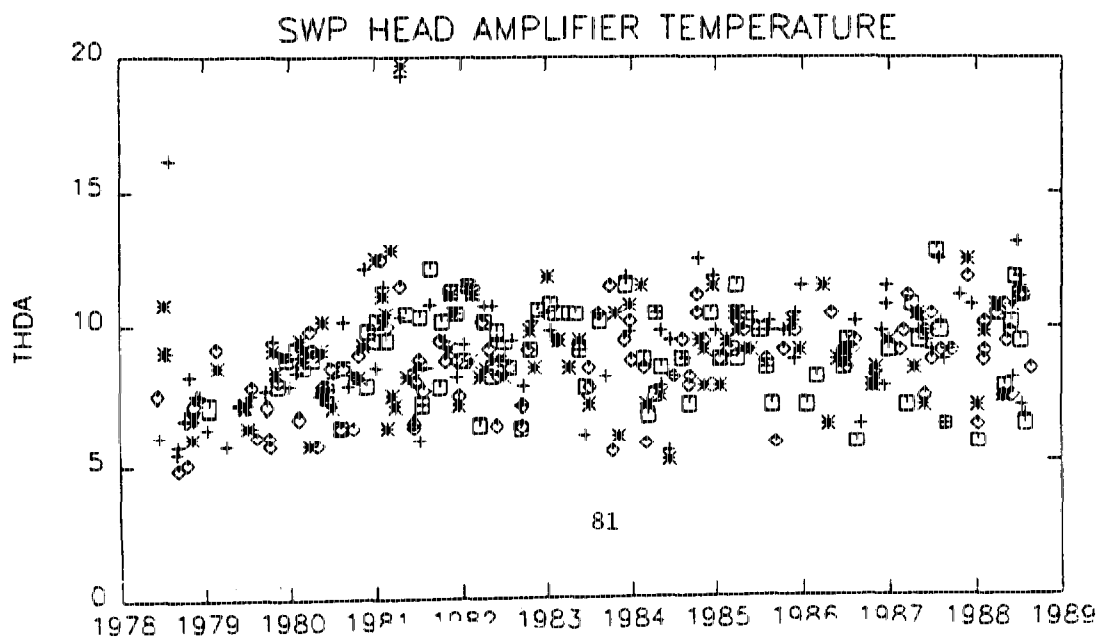
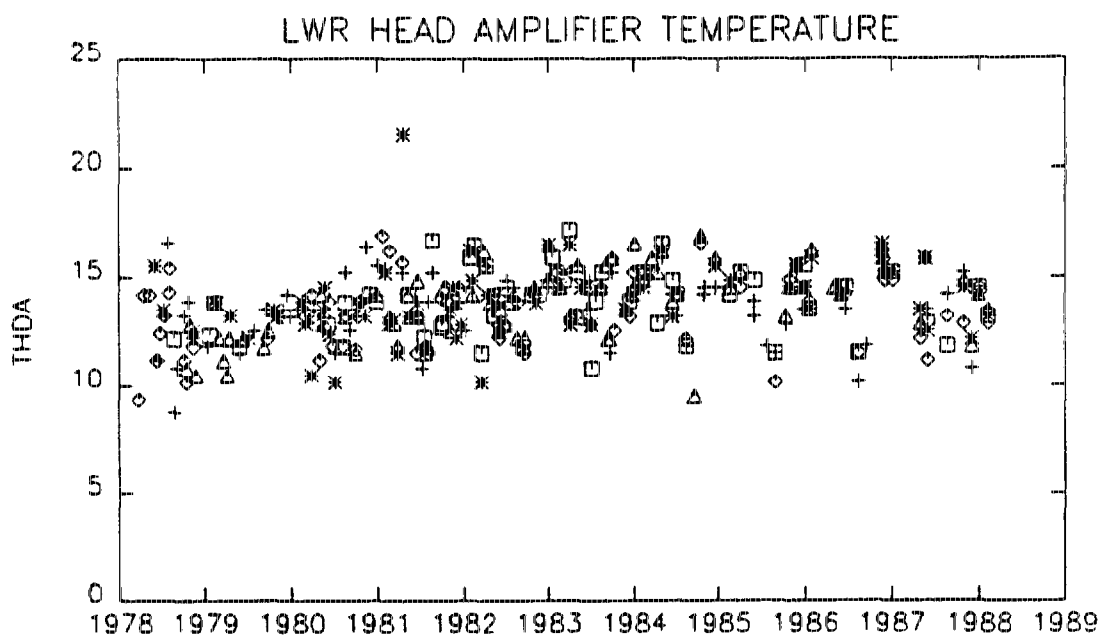


Figure 6.

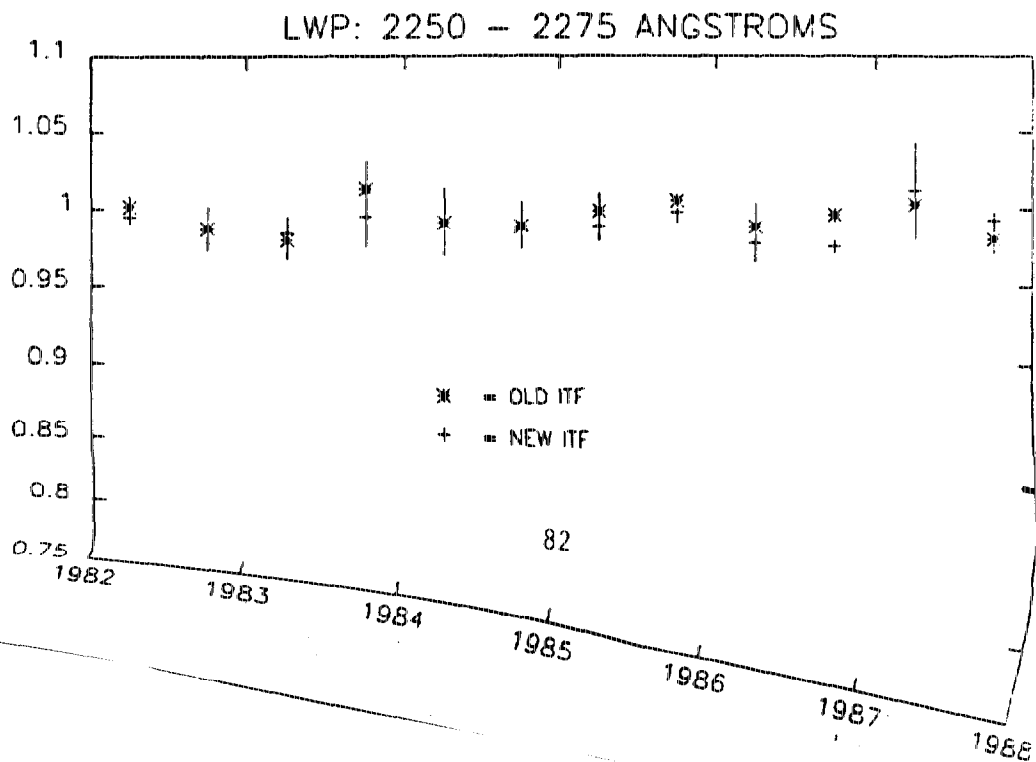
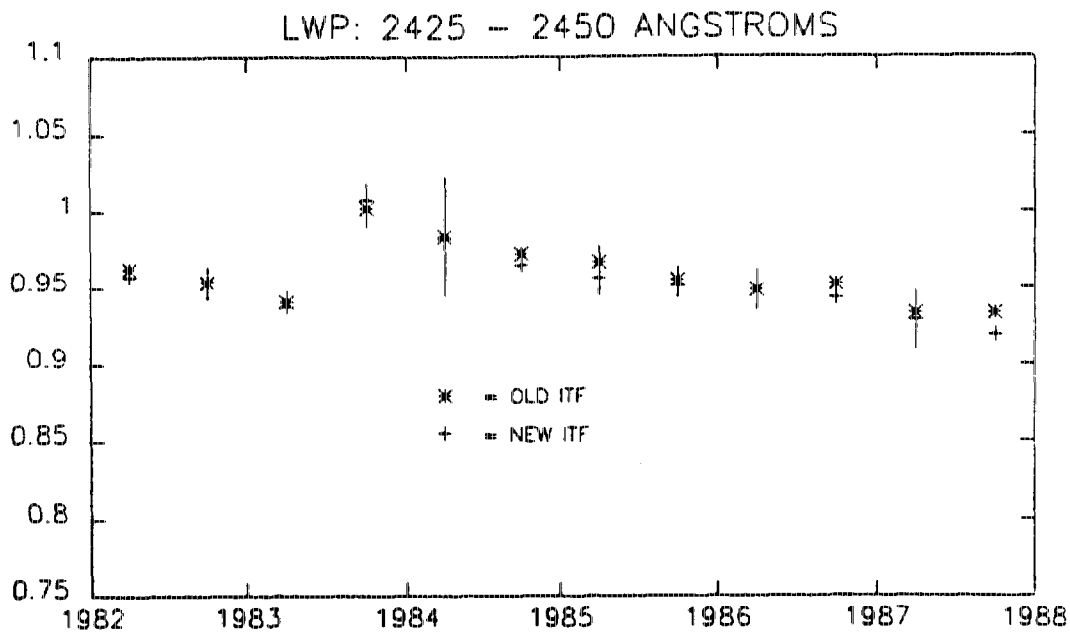
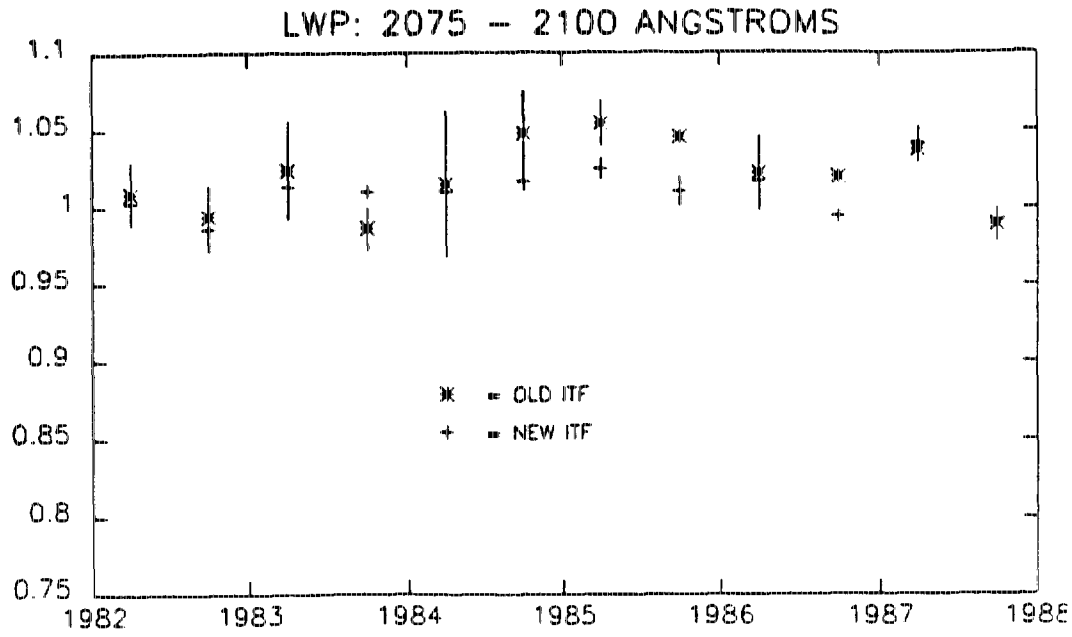


Figure 7.

